Enhancing optical field intensities in Gaussian-profile fiber Bragg gratings

Jeremy Upham,[1,*] Israel De Leon,[1] Dan Grobnic,[2] Edwin Ma,[1] Marie-Claude N. Dicaire,[1] Sebastian A. Schulz,[1] Sangeeta Murugkar,[1] and Robert W. Boyd[1,3]

[1]*Department of Physics, University of Ottawa, Ottawa, ON K1N 6N5, Canada*

[2]*Security and Disruptive Technologies, National Research Council, 100 Sussex Drive, Ottawa, ON K1A 0R6, Canada*

[3]*The Institute of Optics, University of Rochester, Rochester, New York 14627, USA*

**Corresponding author: jupham@uottawa.ca*

Received November 7, 2013; revised December 23, 2013; accepted January 9, 2014; posted January 9, 2014 (Doc. ID 200714); published February 6, 2014

Gaussian profile fiber Bragg gratings exhibit narrow-bandwidth transmission peaks with significant group delay at the edge of their photonic bandgap. We demonstrate group delays ranging from 0.2 to 5.6 ns from a 1.2 cm structure. Simulations suggest such a device would be capable of enhancing the field intensity of incoming light by a factor of 800. Enhancement is confirmed by photothermally induced bistability of these peaks even at sub-milliwatt input powers with as much as a four-fold difference in the magnitude of their responses. The strong field intensities of these modes could significantly enhance desired nonlinear optical responses in fiber, provided the impact of absorption is addressed.

OCIS codes: (060.3735) Fiber Bragg gratings; (190.1450) Bistability; (190.4870) Photothermal effects.
http://dx.doi.org/10.1364/OL.39.000849

Manipulating the grating profile of fiber Bragg gratings (FBGs) is a well-established technique for refining their transmission and reflection features [1,2]. This includes altering the dispersion curve [3] or creating resonant modes [4] to structurally slow down the propagation of light through the device, enhancing local field intensities and nonlinear optical responses [5]. One such FBG profile, the rectified-Gaussian [1,6,7], is drawn schematically in Fig. 1(a). This FBG has a constant Bragg period Λ, while the index modulation Δn has a Gaussian profile along the optical axis of the fiber.

If the index modulation is slowly varying, the local photonic bandgap (PBG) can be solved analytically [7,8]. A larger Δn results in a wider PBG and the Bragg wavelength (λ_B) rises and falls with the mean of Δn. This gives the PBG a "moustache" shape [Fig. 1(b)] and leads to particular transmission characteristics. On the short wavelength side of the PBG light witnesses two reflective regions bounding a propagating mode region. In this spectral range the FBG acts as a Fabry–Perot cavity with multiple resonances, much like a uniform FBG with a DC offset. However, the resonant modes are bound by the PBG, much like the single mode of a pi-phase shift grating. Thus, the rectified-Gaussian FBG exhibits multiple, narrow-bandwidth resonant modes with higher group delays and consequently larger field intensity enhancements (FIEs) [9]. The resulting transmission profile, calculated by the transfer matrix method and overlaid on the PBG in Fig. 1(b), shows a set of such narrow-bandwidth transmission modes in the bounded region.

Experimentally these fine resonant structures were first reported in 1993 [6] and have been shown to exhibit group delays of several nanoseconds [10]. In this work we investigate the relationship between the group delay and FIE of these resonant modes, which could be used to enhance nonlinear optical phenomena in fiber [5]. We also consider how the group delay and enhancement are influenced by the absorption inherent in an FBG [11] and experimentally demonstrate photothermal optical bistability [12,13] at low input powers.

FBGs with the truncated Gaussian design described in Fig. 1 were fabricated in standard SMF-28e fiber by exposing the optical fiber to femtosecond infrared radiation through a phase mask [14]. All reported measurements were taken from a single FBG sample. Normalized transmission and reflection measurements (Fig. 2) were taken with a 100 kHz linewidth, 0.1 pm stepping, continuous wave (CW) laser source at ~7 μW input power and show clear peaks in transmission on the short wavelength side of the PBG. Peaks deeper in the PBG are more tightly

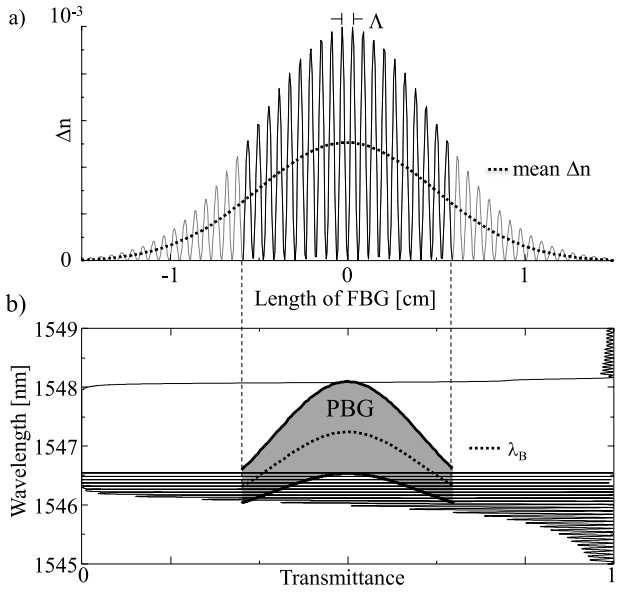

Fig. 1. (a) Gaussian profile FBG (Λ not to scale). The truncated, black region represents the 1.2 cm device under investigation ($\Lambda = 535$ nm, $\Delta n \sim 10^{-3}$, standard deviation = 0.42 cm). (b) Analytic solution of the PBG along the optical axis overlaid with a transfer matrix simulation of the transmittance.

bound so their linewidths are narrower. The narrowest observed transmission line ($\lambda = 1550.6762$ nm) has a FWHM bandwidth of ~0.5 pm (shown in inset of Fig. 2). The linewidths broaden moving away from the center of the PBG: the 9th broadest peak ($\lambda = 1549.9825$ nm) has a bandwidth of 8 pm.

In an ideal system, the normalized transmitted and reflected light would sum to unity over all wavelengths; however, Fig. 2 reveals that some light is unaccounted for at certain wavelengths. While losses on the short wavelength side of the PBG are due to coupling to cladding modes [6], the losses at each resonant peak are attributed to the increased absorption introduced by the FBG writing process [11]. The resonant losses appear to increase as the spectral width decreases. As light is held in these modes longer, a greater portion is absorbed.

To measure the group delay of the resonant peaks, the FBG is introduced into the Mach–Zehnder interferometric system depicted in Fig. 3(a), using the same source as for the transmission measurements. The CW input light is split to create one signal from the sample arm containing the FBG (S) and one from the reference arm (R). The S signal is simply the FBG transmission spectrum [Fig. 3(b) in log scale]. The S and R signals are recombined with a beam splitter and a balanced photodetector isolates the resulting interference component $I(\omega) = \sqrt{SR}[e^{(i\phi(\omega)-i\omega\tau)} + \text{c.c.}]$. The reference arm length is set to be slightly shorter than the sample arm (τ is small, positive). The delay information is contained in the phase difference between S and R, $\phi(\omega)$. Using Fourier transform spectral interferometry [15], the phase argument can be isolated from $I(\omega)$ and its derivative is the group delay, or lifetime, of these optical modes $\tau_g = -(d\phi/d\omega)$ [Fig. 3(c)]. Each peak in transmission has a corresponding jump in group delay due to light being held in resonance. Taking multiple measurements of the peak delays as a whole [Fig. 3(d)] suggests a general increase in delay as the transmission bandwidths narrow. These resonant peaks exhibit delays ranging from 0.2 ± 0.5 ns to 5.6 ± 4.1 ns. The uncertainty in the group delay measurements is ascribed to phase noise between the sample and reference arms from temperature drift and vibrations during measurement. Next we consider the FIE of these resonant modes and how they are impacted by absorption.

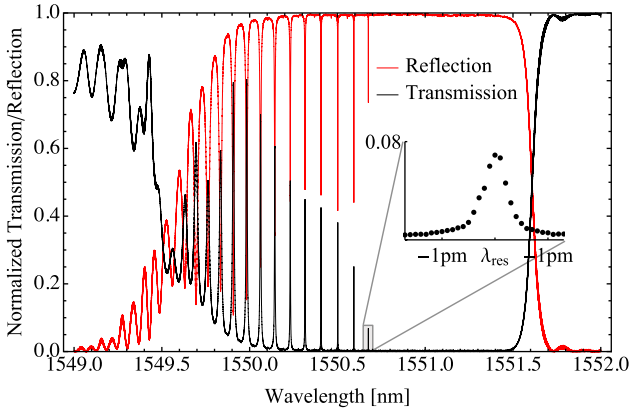

Fig. 2. Experimental transmittance (black) and reflectance (red) data for the Gaussian-profile FBG showing the narrow-bandwidth peaks of the resonant modes. Inset shows that the spectral resolution is sufficient to resolve the narrowest resonant peak.

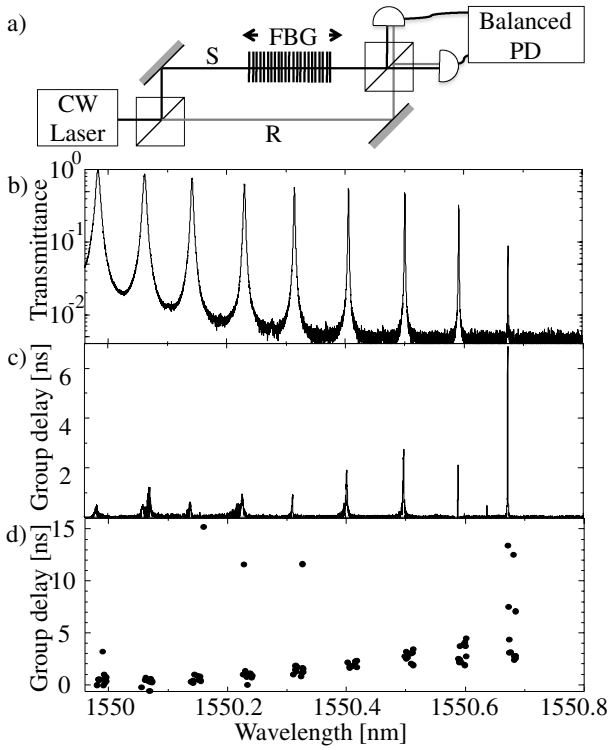

Fig. 3. Measuring group delay in FBGs. (a) Schematic of interferometric measurement setup. (b) Transmittance of the resonance peaks. (c) Group delay measurement. (d) Peak group delays over multiple measurements.

By relating the fraction of light each resonance mode lost to absorption in Fig. 2 to its measured group delay, we estimate the rate of absorption for light in the FBG region to be $5.4 \pm 1.7 \times 10^7$ s^{-1}. Assuming that the same absorption applies to wavelengths of light passing through the 1.2 cm FBG without interacting with the grating, we estimate the broadband, nonresonant absorption induced in the fiber core by the grating writing process to be $\alpha = 0.25 \pm 0.17$ m^{-1} (0.057 ± 0.040 dB/cm), which is in keeping with FBGs with similar Δn in SMF-28 [10].

Figure 4(a) shows a close up of the six lowest-order transmission peaks simulated by the transfer matrix method with (black) and without (red) this estimated absorption. Without absorption the linewidths of these peaks range from 0.001 pm for peak F up to 2 pm for peak A, while introducing absorption strongly suppresses the lowest-order modes. Figure 4(b) shows the FIE of each mode, relative to the incident CW source. Figure 4(c) relates the enhancement of the field intensity to the group delay, which is calculated from the phase of the transmitted light.

Without absorption, the FIE is very large for modes that lie deeper within the PBG, but realistically the absorption losses will also increase as light is confined to these modes for longer time, placing an upper bound on the enhancement that can be achieved in these resonant modes. Comparing these simulations to the measurements in Fig. 3(d) suggests that optimal enhancement of the input light might not occur at the

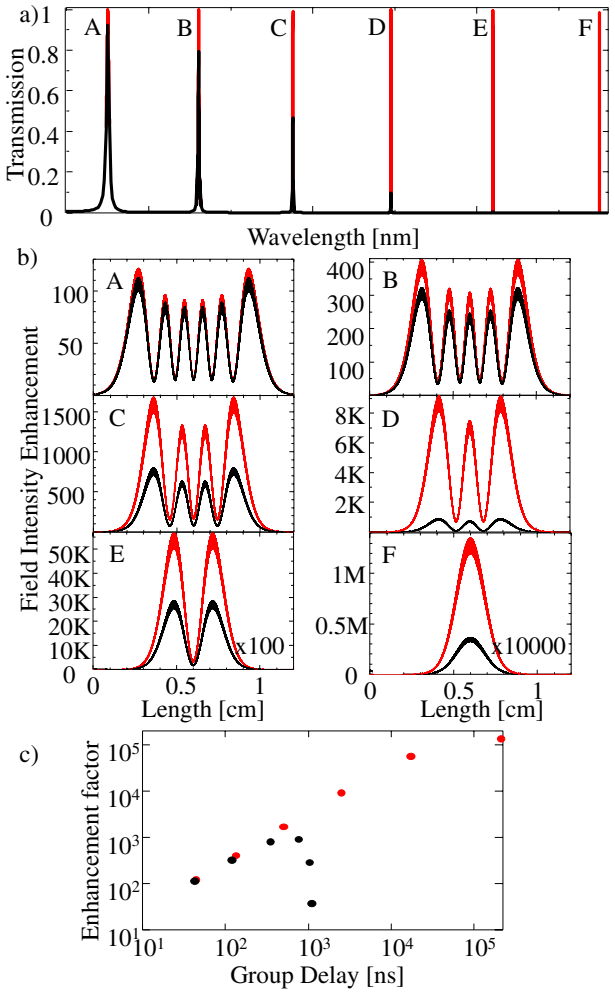

Fig. 4. Transfer matrix method simulations of FBG resonant modes with (black) and without (red) absorption. (a) The transmission spectrum. (b) FIE for each resonant mode. (c) Relationship between FIE and group delay showing enhancements of ~800 seem achievable even with absorption.

lowest-order modes, but rather those modes where the FIE is not yet overpowered by absorption. Experimentally, we are likely not even observing the lowest-order modes of our device, as absorption attenuates their transmission below the noise floor. Absorption similarly limits enhancement in other FBG designs considered for nonlinear applications [9].

In principle, pi-phase shift FBGs should be capable of significantly larger FIE than rectified Gaussians. While not optimized for that purpose, the largest FIE values estimated from experimental results on pi-phase shift gratings are 19 in [16] and 45 in [17]. By comparison, this Gaussian profile FBG appears capable of enhancing field intensities by a factor of ~800 [Fig. 4(c)]. Improvements to this Gaussian profile FBG, designed to limit the impact of absorption, could presumably lead to further enhancements in realistic devices.

Having confirmed the presence of resonant modes with large group delays in this FBG structure and estimated the resulting FIE, we seek experimental confirmation of this optical enhancement. To do so we evaluate the pronounced response of the different resonant modes to small increases in input power. Figure 5 shows

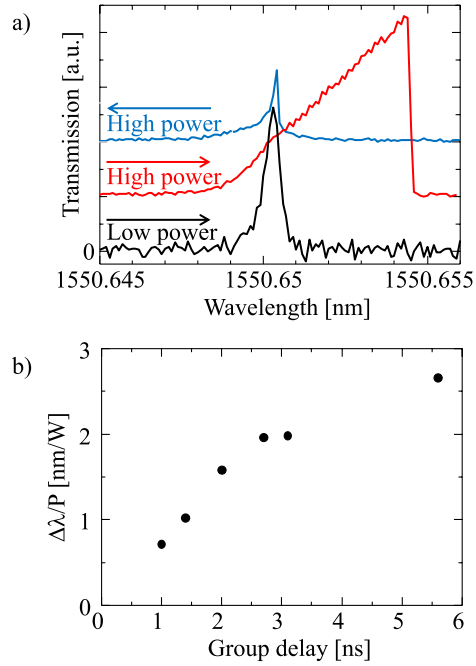

Fig. 5. Demonstration of optical bistability induced by the thermo-optic effect at small input powers. (a) For the sharpest observed resonant peak, low input power is 7 μW, while high is 340 μW. Plots vertically offset for clarity. (b) Measured wavelength shift response to input power for resonant modes of different group delay.

the transmission responses of a single resonant mode to three different CW spectral sweeps: increasing wavelength at low (~7 μW) input power, increasing wavelength at higher (340 μW) input power, and decreasing wavelength, also at 340 μW. Note that these sub-milliwatt powers are very small to be observing nonlinear responses in a standard fiber. At low input powers (black), a spectral sweep produces a linear response. The path dependency of the resonant mode and sharp discontinuities in the spectrum at stronger input powers indicate optical bistability [13], caused by local heating of the FBG by the photothermal effect [18]. Consider when a high input power CW light is swept in increasing wavelength (red). As the input light begins to couple to the short wavelength side of the resonator, the fields begin to build up in the mode and are partially absorbed. The resulting heat increases the refractive index of the fiber and shifts the resonant mode to higher wavelengths. As the input wavelength increases further, the buildup of light in the mode and consequent heating "pushes" the resonant peak to higher wavelengths, creating a sloped line on one side of the transmission peak. Eventually the incident light's wavelength catches up to the shifted resonant wavelength of the mode. Here, the FIE has reached its maximum, resulting in the largest wavelength shift for this mode at this input power. The next step in the laser wavelength reduces the field intensity, resulting in less absorption. The resonant mode relaxes to its original wavelength as it cools, producing a discontinuous drop in transmission. The blue line shows the resonant mode response to the same probe light decreasing in wavelength. As the light begins to couple to the mode, the heating pulls the resonator toward it, creating a

smaller but still observable discontinuity. As the light continues decreasing in wavelength, the mode relaxes with it, giving a gradual slope on the low wavelength side of the mode.

The relatively slow response of the photothermal effect in FBGs [18], ~30 μs in our system, makes it a generally undesirable nonlinear optical response [11] compared to the faster but more subtle optical Kerr effect [16,17]. However, the ~5 pm photothermal shift induced by a sub-milliwatt CW input supports the idea that the optical fields are being strongly confined, and their intensities strongly enhanced, within the resonator. Because the amount of heat produced depends on how strong the fields of the mode can be built up and consequently absorbed, larger photothermal shift for the same incident CW power is an indicator of larger FIE. As the Gaussian profile FBG has multiple modes of different group delay, the relative magnitude of photothermal shifts of the resonant modes for the same incident power is a measure of their relative field enhancements. Figure 5(b) plots the strength of this bistable response as wavelength shift per incident light power versus group delay for the six narrowest transmission lines. The roughly proportional increase of photothermal response to group delay supports our claim that the narrower the modes, the higher the FIE. The fact that any of these modes showed a measurable response at sub-milliwatt input powers suggests this enhancement is large. Optical modes exhibiting large FIE have the potential to enhance various desired nonlinear optical phenomena, such as self-phase modulation and four-wave mixing, that might otherwise require strong input powers, specialized fiber cross sections, or exotic nonlinear materials [5]. If the confinement of light within the resonant modes is strong enough to exhibit thermo-optically induced bistability even at these low input powers, then these resonances hold potential for the enhancement of other nonlinear processes.

In summary, the rectified Gaussian FBG profile has the potential to significantly enhance optical field intensities within optical fiber modes and as such, shows potential for various nonlinear optical applications. By considering a sample with measurable group delays up to 5.6 ns, we estimate the resulting enhancement of the field intensities and how this is impacted by the absorption losses introduced in the FBG writing process. Even accounting for losses, simulations estimate a FIE factor of 800 in some resonant modes. Thermo-optically induced bistability observed at sub-milliwatt input powers suggests that the FIEs are sufficient in multiple resonant modes to provide opportunities for nonlinear phenomena involving multiple wavelengths, such as four-wave mixing. The resonant modes themselves also merit deeper study. While these transmission peaks in the PBG consist of Fabry–Perot-like resonances bound by two finite bandgap regions, the propagation modes between the two reflectors could be slowed by dispersion near the edge of the PBG. Further investigation into nonuniform FBGs profiles could yet reveal even more opportunities for fiber-based nonlinear optics.

The research was supported by the Canada Excellence Research Chairs (CERC) program.

References

1. T. Erdogan, J. Lightwave Technol. **15**, 1277 (1997).
2. C. R. Giles, J. Lightwave Technol. **15**, 1391 (1997).
3. J. Khurgin, Phys. Rev. A **62**, 013821 (2000).
4. G. P. Agrawal and S. Radic, IEEE Photon. Technol. Lett. **6**, 995 (1994).
5. R. W. Boyd, J. Opt. Soc. Am. B **28**, A38 (2011).
6. V. Mizrahi and J. Sipe, J. Lightwave Technol. **11**, 1513 (1993).
7. J. E. Sipe, L. Poladian, and C. M. de Sterke, J. Opt. Soc. Am. A **11**, 1307 (1994).
8. L. Poladian, Opt. Lett. **22**, 1571 (1997).
9. I. V. Kabakova, T. Walsh, C. M. de Sterke, and B. J. Eggleton, J. Opt. Soc. Am. B **27**, 1343 (2010).
10. H. Wen, M. Terrel, S. Fan, and M. Digonnet, IEEE Sens. J. **12**, 156 (2012).
11. I. C. M. Littler, T. Grujic, and B. J. Eggleton, Appl. Opt. **45**, 4679 (2006).
12. H. G. Winful, J. H. Marburger, and E. Garmire, Appl. Phys. Lett. **35**, 379 (1979).
13. H. M. Gibbs, *Optical Bistability: Controlling Light with Light* (Academic, 1985).
14. D. Grobnic, C. W. Smelser, S. J. Mihailov, and R. B. Walker, IEEE Photon. Technol. Lett. **16**, 1864 (2004).
15. A. Gomez-Iglesias, D. O'Brien, L. O'Faolain, A. Miller, and T. Krauss, Appl. Phys. Lett. **90**, 261107 (2007).
16. I. V. Kabakova, B. Corcoran, J. A. Bolger, C. M. de Sterke, and B. J. Eggleton, Opt. Express **17**, 5083 (2009).
17. I. V. Kabakova, C. M. de Sterke, and B. J. Eggleton, J. Opt. Soc. Am. B **27**, 2648 (2010).
18. J. H. Chow, B. S. Sheard, D. E. McClelland, and M. B. Gray, Opt. Lett. **30**, 708 (2005).